



Project:  
**GEOCARBON**

Project full title:  
***Operational Global Carbon Observing System***

European Commission - FP7  
Collaborative Project (large scale integrating project) - for specific  
cooperation actions (SICA) dedicated to international cooperation partner countries  
Grant agreement no.: **283080**

**Del. no: 6.3**

**Deliverable name: Synthesis of the global carbon flux estimates from atmospheric inversions**

Version: V1

WP no: 6

Lead beneficiary: LSCE-UVSQ

Delivery date from Annex I (project month): 18

Actual delivery date (project month): 18

---

## **1. Introduction**

### *1.1 Short summary*

Atmospheric CO<sub>2</sub> inversions estimate surface carbon fluxes from an optimal fit to atmospheric CO<sub>2</sub> measurements, usually including prior constraints on the flux estimates. Eleven sets of carbon flux estimates are compared, generated by different inversions systems that vary in their inversions methods, choice of atmospheric data, transport model and prior information. The inversions were run for at least 5 years in the period between 1990 and 2009. Mean fluxes for 2001-2004, seasonal cycles, interannual variability and trends are compared for the tropics and northern and southern extra-tropics, and separately for land and ocean as well as for some continental/basin-scale subdivisions. Four-year mean fluxes are reasonably consistent across inversions at global/latitudinal scale, with a large total (land plus ocean) carbon uptake in the north ( $-3.3 \text{ PgCy}^{-1}$  ( $\pm 0.6$  standard deviation)) nearly equally spread between land and ocean, a significant although more variable source over the tropics ( $1.6 \pm 1.0 \text{ PgCy}^{-1}$ ) and a compensatory sink of similar magnitude in the south ( $-1.4 \pm 0.6 \text{ PgCy}^{-1}$ ) corresponding mainly to an ocean sink. Largest differences across inversions occur in the balance between tropical land sources and southern land sinks. Interannual variability (IAV) in carbon fluxes is larger for land than ocean regions (standard deviation around  $1.05$  versus  $0.34 \text{ PgCy}^{-1}$  for the 1996-2007 period), with much higher consistency among the inversions for the land. While the tropical land explains most of the IAV (stdev $\sim 0.69 \text{ PgCy}^{-1}$ ), the northern and southern land also contribute (stdev $\sim 0.39 \text{ PgCy}^{-1}$ ). Most inversions tend to indicate an increase of the northern land carbon uptake through the 2000s (around  $0.11 \text{ PgCy}^{-1}$ ), shared by North America and North Asia. The mean seasonal cycle appears to be well constrained by the

atmospheric data over the northern land (at the continental scale), but still highly dependent on the prior flux seasonality over the ocean.

Note finally that the results presented here are the latest comprehensive intercomparison and that this effort was launched with the RECCAP initiative (REgional Carbon Cycle Assessment and Processes, Canadell et al., 2011) as part of the international Global Carbon Project (<http://www.globalcarbonproject.org/reccap/>). The re-formatted files are available under the TRANSCOM web site: «<http://transcom.lsce.ipsl.fr/>» for 3D flux fields (longitude, latitude, time) as well as for regional aggregate s(region, time) given an ensemble of pre-defined land eco-regions and ocean basins.

These results will be published in Biogeosciences (Peylin et al. 2013, under review).

### *1.2 Rationale for this deliverable*

The synthesis of surface carbon fluxes from “standard” atmospheric inversion is critical for the GEOCARBON project. It will provide flux estimates to compare with the results of component 2 (WP-9-10-13) based on Carbon Cycle Data Assimilation Systems (CCDAS). CCDASs provide a mean to assimilate different carbon cycle data streams, including atmospheric CO<sub>2</sub> concentrations, through the optimisation of key parameters of process-based models of the land/ocean carbon cycle. Atmospheric inversion and CCDAS flux estimates are thus complementary, in the sense that:

- CCDAS fluxes offer the possibility to include other data streams than just atmospheric CO<sub>2</sub> observations.
- CCDAS fluxes deeply rely on the structure of the model that is used, bringing additional information to the optimisation procedure. This information allows spreading in space and time the sparse information from current atmospheric CO<sub>2</sub> networks, but in the mean time imposes a strong constraint on the estimated fluxes.
- Reversely, atmospheric inversions close the year-to-year budget of recently observed CO<sub>2</sub> increase in the atmosphere without specific model structure limitation like for the CCDAS systems (i.e., missing processes).
- CCDAS results provide a comprehensive picture of the global/continental carbon fluxes and stocks and insights on the processes controlling the flux variability, while atmospheric inversions only inform on the net fluxes.

The atmospheric inversion synthesis will thus be directly used in WP13 for the synthesis of the CCDAS results, as additional flux estimates providing “partly independent” information.

### *1.3 Problems encountered and envisaged solutions*

No specific problems were encountered.

## **2 Full description**

### *2.1 Selected Atmospheric inversions and post-processing*

The LSCE Laboratory has been collecting carbon flux estimates from state-of-the-art inversions performed by groups around the world in an effort to construct a new atmospheric CO<sub>2</sub> inversion intercomparison. The results of these inversions are currently displayed through a web-site (<https://transcom.lsce.ipsl.fr/>), and represent 14 different approaches. For the purpose of satisfying the RECCAP inter-comparison project, eleven of the submissions to LSCE were selected (Table 1)

for an in-depth intercomparison. We restricted the selection to inversions that span a time period of at least 5 years. The participating submissions reflect a range of choices for atmospheric observations, transport model, spatial and temporal flux resolution, prior fluxes, observation uncertainty and prior error assignment, as well as inverse method.

Table 1. Participating inversion systems and key attributes.

Acronym	Reference	# of regions	Time Period	Obs <sup>1</sup>	# of obs locations <sup>2</sup>	IAV <sup>3</sup> wind	IAV <sup>4</sup> priors
LSCEa	Piao et al, 2009	Grid-cell (96x72)	1996-2004	MM	67	Yes	No
LSCEv (v1.0)	Chevallier et al, 2010	Grid-cell (96x72)	1988-2008	Raw	128	Yes	Yes
CCAM	Rayner et al, 2008	146	1992-2008	MM	73 CO <sub>2</sub> 7 $\delta^{13}\text{CO}_2$	No	No
MATCH	Rayner et al, 2008	116	1992-2008	MM	73 CO <sub>2</sub> 7 $\delta^{13}\text{CO}_2$	No	No
CT2009	Peters et al, 2007	156	2001-2008	Raw	94	Yes	Yes
CTE2008	Peters et al, 2010	168	2001-2007	Raw	117	Yes	Yes
JENA (s96, v3.3)	Rödenbeck, 2005	Grid-cell (72x48)	1996-2009	Raw	53	Yes	No
RIGC (TDI-64)	Patra et al, 2005a	64	1989-2008	MM	74	Yes	No
JMA	Maki et al, 2010	22	1985-2009	MM	146	Yes	No
TrC	Gurney et al, 2008	22	1990-2008	MM	103	No	No
NICAM	Niwa et al, 2012	40	1988-2007	MM	94	Yes	No

1: Observations used as monthly means (MM) or at sampling time (Raw)

2: Number of measurement locations included in the inversion (some inversions use multiple records from a single location)

3: Inversion accounts for interannually varying transport (Yes) or not (No)

4: Inversion accounts for interannually varying prior fluxes (Yes) or not (No)

The results reported by the different participants were resampled onto a common 1° x 1° grid to facilitate more direct comparisons between the estimated fluxes. Once re-gridded, the results have been aggregated i) to land and ocean regions consistent with the RECCAP regional divisions described in Canadell et al. (2011) and ii) to larger scale totals (northern land, tropical ocean, etc). However, significant differences in prescribed fossil fuel emissions complicated the intercomparison of the estimated “natural” fluxes. In order to minimize this problem, we chose to “adjust” the natural land/ocean fluxes in order to account for these differences. We thus took the total surface-to-atmosphere gridded flux from each inversion and subtracted a common fossil fuel flux in order to obtain “fossil corrected” natural land and ocean components. For the reference fossil fuel emission, we took the recent annual gridded fluxes from EDGARv4.2.

## 2.2 Results: Comparison of the inversion fluxes

### Long-term mean fluxes:

The long-term mean fluxes are defined for the 2001-2004 period, common to all inversions, and displayed in figure 1. The land and ocean (fossil corrected) have similar values for global uptake, with the mean flux and standard deviation across inversions giving around  $-1.46 \pm 0.55$  and  $-1.63 \pm 0.49$  PgCy<sup>-1</sup>, for land and ocean respectively. The exceptions are the JENA submission, which has much larger uptake on land and smaller uptake by the ocean (both compensating), and NICAM which gives the smallest land uptake compensated by the largest ocean sink.

When analyzed in latitudinal bands, the mean “natural” flux across the inversions results in a large total (land plus ocean) sink in the north ( $-3.3 \pm 0.6$  PgCy<sup>-1</sup>), a significant source over the tropics ( $1.6 \pm 1.0$  PgCy<sup>-1</sup>) and a compensatory sink of similar magnitude in the south ( $-1.4 \pm 0.6$  PgCy<sup>-1</sup>). The

spread between the different inversions at the scale of latitudinal bands is still relatively large. In the north, the LSCEv system estimates the smallest total carbon uptake ( $-2.5 \text{ PgCy}^{-1}$ ), while RIGC gives the largest uptake ( $-4.4 \text{ PgCy}^{-1}$ ). The spread among the inversions is much greater in the tropics with a standard deviation close to  $1 \text{ PgCy}^{-1}$ , reflecting, in part, the low density of atmospheric stations in this region. In the south, the spread obtained for the total flux is comparable to the north ( $\sigma$  values are slightly less than  $0.6 \text{ PgCy}^{-1}$  for both north and south regions). Finally, the division of the total natural fluxes (fossil corrected) from each latitude band into land and ocean components (second and third column of Fig. 1) shows that:

- In the north, the land natural sink appears to be twice as large as the ocean sink with a significant spread across the inversions.
- In the tropics, all inversions tend to produce a similar ocean carbon source of around  $0.8 \text{ PgCy}^{-1}$  with a relatively small spread ( $\sigma=0.2 \text{ PgCy}^{-1}$ ). Such a value does not significantly deviate from the prior ocean fluxes used by the inversions, mostly based on one of Takahashi et al. (1999, 2009) climatologies.
- In the south, all inversions produce a large ocean carbon uptake, with a flux around  $-1.3 \text{ PgCy}^{-1}$  and a relatively small spread. Over land, the inversions do not agree on the sign of the natural flux, varying from  $-0.9$  to  $+0.4 \text{ PgCy}^{-1}$ .

Finally, we considered the breakdown of the northern hemisphere into continental regions (North America, Europe and Eurasia, figure not shown). The three land regions show a significant carbon sink, with fluxes from  $-0.4 \text{ PgCy}^{-1}$  over Europe to  $-1.0 \text{ PgCy}^{-1}$  over North Asia. A large spread among the inversions remains with standard deviations of up to  $0.5 \text{ PgCy}^{-1}$  for each region. When differences in surface area are accounted for Europe exhibits the greatest land uptake ( $-41 \text{ gCm}^{-2}\text{y}^{-1}$ ) and North Asia the smallest ( $-27 \text{ gCm}^{-2}\text{y}^{-1}$ ).

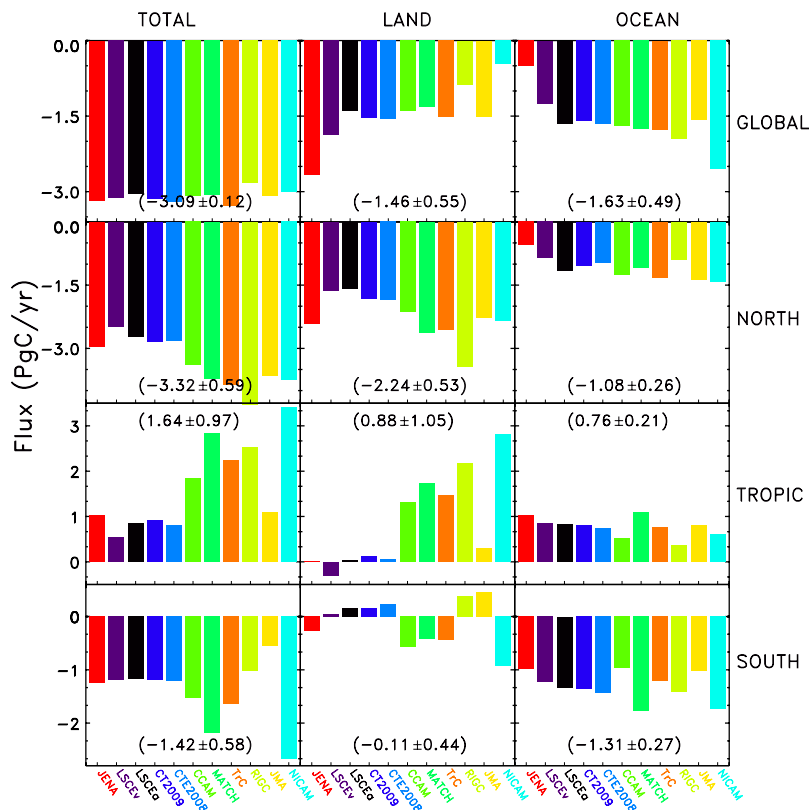


Figure 1: Mean natural fluxes for the period 2001-2004 of the individual participating inversion posterior fluxes. Shown here are total (first column), natural “fossil corrected” land (second column) and natural ocean (third column) carbon

exchange aggregated over the Globe (top row), the North (2<sup>nd</sup> row), the Tropics (3<sup>rd</sup> row) and the South (bottom row), with the three regions divided by approximately 25°N and 25°S. Numbers in parentheses represent the mean flux and the standard deviation across all inversions.

#### Inter-annual variability:

Figure 2 shows the interannual variability (IAV) for the northern, tropical and southern aggregated land and ocean regions. All submissions tend to exhibit greater IAV on land versus ocean, particularly in the tropical latitude band. For the 1996-2007 period, the mean across all inversions of the standard deviation of the annual means over land is around 1.05 PgCy<sup>-1</sup> versus 0.34 PgCy<sup>-1</sup> over the ocean. Over land, we obtain 0.69 PgCy<sup>-1</sup> for the tropics and only 0.39 PgCy<sup>-1</sup> for both northern and southern land. This is consistent with i) numerous inversion studies over the past two decades (e.g. Bousquet et al., 2000, Baker et al., 2006) and ii) several analysis of land ecosystem model results (i.e., Sitch et al. 2008) and ocean model results (i.e., Le Quere et al., 2000, 2010). Note also that it may reflect in part the tighter prior constraint most inversions apply to ocean regions relative to the land. Within the land aggregates, the tropical land exhibits the greatest amount of interannual variability while for the oceans, greater interannual variability is seen in the southern ocean (mainly associated with the 1997/1998 time period).

The phasing of the carbon exchange anomalies shows consistency among the inversion submissions. Positive global land anomalies across the submissions occur for the following years: 1995, 1997/1998, 2002/2003, 2005/2006, and 2007/2008. All of these positive anomalies appear to be driven by the tropical land region though the 2002/2003 anomaly shows potential contributions from the northern and southern land as well. Ocean interannual variability shows less consistency among the inversions.

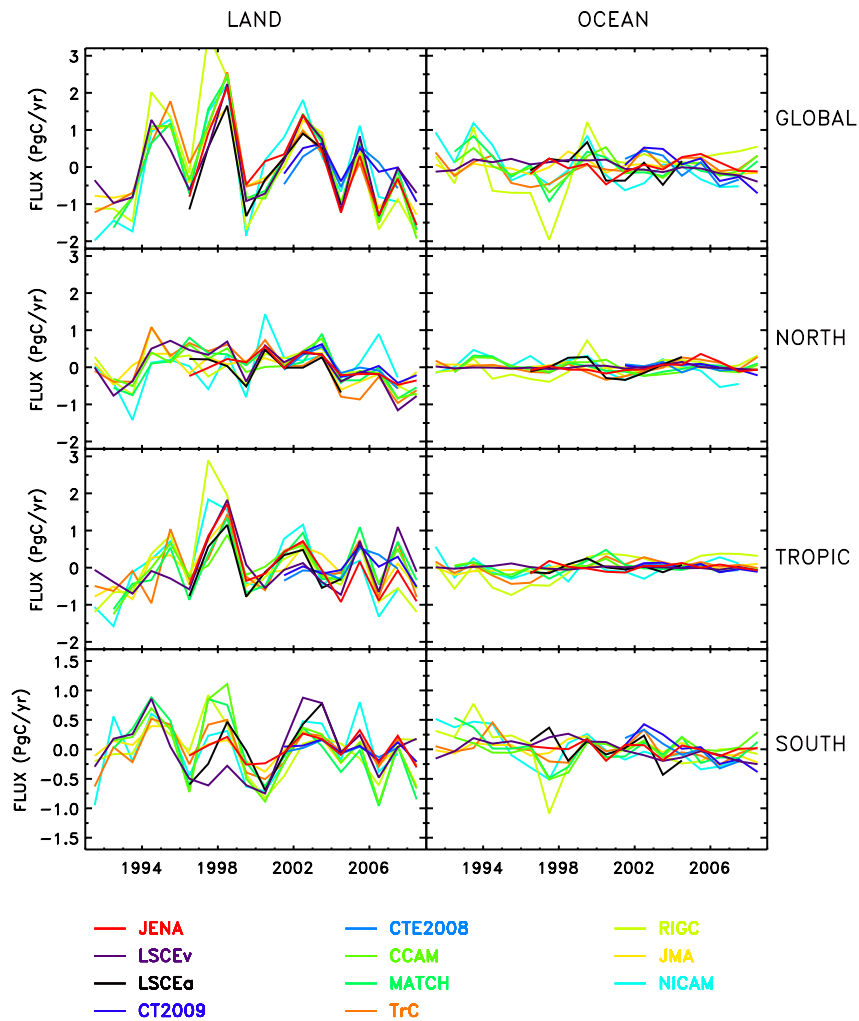


Figure 2: Annual mean anomalies of the individual participating inversion posterior flux estimates. Shown here are the fossil corrected natural land (first column) and natural ocean (second column) carbon exchange for the Globe (top row), the North (2<sup>nd</sup> row), the Tropics (3<sup>rd</sup> row) and the South (bottom row), with the three regions divided by approximately 25°N and 25°S.

### Long-term trends:

Long-term trends are difficult to determine from this set of inversions because of relatively short record and large inter-annual variations. Figure 3 divides the northern land into regions, showing the three-year smoothed fluxes for North America, Europe and North Asia. The figure shows a tendency towards increasing land uptake for North America and Asia over most of the last decade (around 1 PgC), while the European uptake is relatively constant. The trend appears to be slightly larger over North Asia than North America, and for this latter region two inversions show contrasting results (NICAM and JMA). However, these are all regions with significant fossil fuel CO<sub>2</sub> emissions and it is important to understand how these trends could be influenced by how each inversion includes fossil emissions and how the results may be influenced by the fossil correction applied to the results.

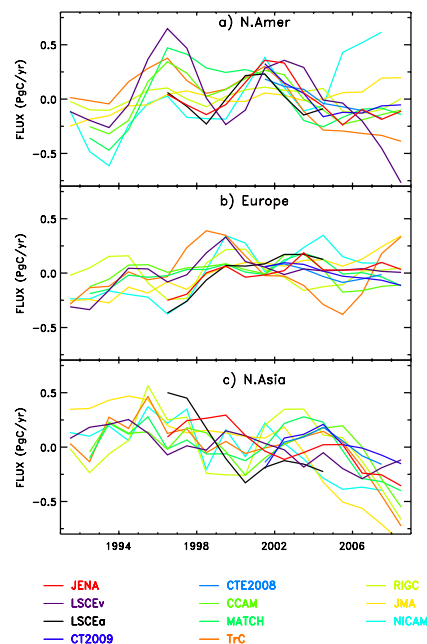


Figure 3: Smoothed annual mean (smoothing window of 3 years) carbon exchange from the individual participating inversions aggregated over a) North America, b) Europe, and c) North Asia.

#### Mean seasonal cycle:

The global land seasonality is driven by the northern land with close agreement regarding both the magnitude and phasing of the growing season and dormant season fluxes. For northern land, the amplitude of the seasonal cycle is close to 3 PgC/month (CT having the smallest amplitude with 2.8 PgC/month and NICAM the largest with 3.6 PgC/month) and the peak of the growing season is located in July for all inversions. The growing season shows a larger spread across the inversions than the dormant season. Northern ocean flux seasonal cycles show less agreement in both phase and magnitude across the inversions. Since the amplitude of the northern ocean seasonality is much smaller than that of the land, a small error in the allocation of seasonality between land and ocean regions can more easily change the phase of the estimated ocean seasonality between inversions than that of the land seasonality.

Seasonality for the tropical land is smaller than the northern land with most inversions giving maximum uptake around August to October. The seasonality of the tropical oceans shows much smaller amplitude than the tropical land and with less agreement in phase and magnitude.

Seasonality in the Southern Land shows reasonable consistency across the inversions in terms of phasing. Maximum carbon uptake across the inversions spans the February to April time period. The peak of the dormant season carbon emission varies from June to October depending upon the inversion. Southern ocean fluxes show general agreement with uptake in the Austral Winter/Spring, opposing the seasonality of the southern land.

### 3 References

Baker, D. F., Law, R. M., Gurney, K. R., Rayner, P., Peylin, P., Denning, A.S., Bousquet, P., Bruhwiler, L., Chen, Y.-H., Ciais, P., Fung, I. Y., Heimann, M., John, J., Maki, T., Maksyutov, S., Masarie, K., Prather, M., Pak, B., Taguchi, S., and Zhu, Z.: TransCom 3 inversion intercomparison:

Impact of transport model errors on the interannual variability of regional CO<sub>2</sub> fluxes, 1988–2003, *Global Biogeochem. Cycles*, 20, GB1002, doi:10.1029/2004GB002439, 2006.

Bousquet, P., Peylin, P., Ciais, P., Le Quéré, C., Friedlingstein, P., and Tans, P. P.: Regional Changes in Carbon Dioxide Fluxes of Land and Oceans Since 1980, *Science*, 290, 1342-1346, doi: 10.1126/science.290.5495.1342,2000.

Canadell, J. G., Ciais, P., Gurney, K., Le Quéré, C., Piao, S., Raupach, M.R., and Sabine, C. L.: An International Effort to Quantify Regional Carbon Fluxes, *Eos Trans. AGU*, 92(10), 81, doi:10.1029/2011EO100001, 2011.

Chevallier, F., Ciais, P., Conway, T.J., Aalto, T., Anderson, B. E., Bousquet, P., Brunke, E. G., Ciattaglia, L., Esaki, Y., Fröhlich, M., Gomez, A. J., Gomez-Pelaez, A. J., Haszpra, L., Krummel, P., Langenfelds, R., Leuenberger, M., Machida, T., Maignan, F., Matsueda, H., Morguí, J. A., Mukai, H., Nakazawa, T., Peylin, P., Ramonet, M., Rivier, L., Sawa, Y., Schmidt, M., Steele, P., Vay, S. A., Vermeulen, A. T., Wofsy, S., and Worthy, D.: CO<sub>2</sub> surface fluxes at grid point scale estimated from a global 21 year reanalysis of atmospheric measurements, *J. Geophys. Res.*, 115, D21307, doi:10.1029/2010JD013887, 2010.

Gurney, K. R., Baker, D., Rayner, P., and Denning, S., Interannual variations in continental-scale net carbon exchange and sensitivity to observing networks estimated from atmospheric CO<sub>2</sub> inversions for the period 1980 to 2005, *Global Biogeochem. Cycles*, 22, GB3025, doi:10.1029/2007GB003082, 2008.

Le Quéré, C., Orr, J., Monfray, P., Aumont, O., and Madec, G.: Interannual variability of the oceanic sink of CO<sub>2</sub> from 1969 to 1997, *Global Biogeochem. Cycles*, 22, GB3009, 2000.

Le Quéré, C., Takahashi, T., Buitenhuis, C. E., Rödenbeck, C., and Sutherland, S.: Impact of climate change on the global oceanic sink of CO<sub>2</sub>. *Global Biogeochem. Cycles*, 24, GB4007, 2010.

Maki, T., Ikegami, M., Fujita, T., Hirahara, T., Yamada, K., Mori, K., Takeuchi, A., Tsutsumi, Y., Suda, K. and Conway, T. J., New technique to analyse global distributions of CO<sub>2</sub> concentrations and fluxes from non-processed observational data. *Tellus B*, 62, 797–809. doi: 10.1111/j.1600-0889.2010.00488.x, 2010.

Niwa, Y., Machida, T., Sawa, Y., Matsueda, H., Schuck, T. J., Brenninkmeijer, C. A. M., Imasu, R., and Satoh, M., Imposing strong constraints on tropical terrestrial CO<sub>2</sub> fluxes using passenger aircraft based measurements, *J. Geophys. Res.*, 117, D11303, doi:10.1029/2012JD017474, 2012.

Patra, P. K., Maksyutov, S., Ishizawa, M., Nakazawa, T., Takahashi, T. and Ukita, J.: Interannual and decadal changes in the sea-air CO<sub>2</sub> flux from atmospheric CO<sub>2</sub> inverse modelling, [Global Biogeochem. Cycles](#), 19, GB4013, 2005a.

Peters, W., Jacobson, A. R., Sweeney, C., Andrews, A. E., Conway, T. J., Masarie, K., Miller, J. B., Bruhwiler, L., M. P., Pétron, G., Hirsch, A. I., Worthy, D. E. J., van der Werf, G. R., Randerson, J. T., Wennberg, P. O., Krol, M. C., and Tans, P.P.: An atmospheric perspective on North American carbon dioxide exchange: CarbonTracker, *PNAS*, 104, 18925-18930, doi:10.1073/pnas.0708986104, 2007.

Peters, W., Krol, M. C., van der Werf, G. R., Houweling, S., Jones, C. D., Hughes, J., Schaefer, K., Masarie, K. A., Jacobson, A. R., Miller, J. B., Cho, C.H., Ramonet, M., Schmidt, M., Ciattaglia, L., Apadula, F., Heltai, D., Meinhardt, F., Di Sarra, A. G., Piacentino, S., Sferlazzo, D., Aalto, T., Hatakka, J., Ström, J., Haszpra, L., Meijer, H. A. J., Van der Laan, S., Neubert, R. E. M., Jordan, A., Rodó, X., Morguí, J.-A., Vermeulen, A. T., Popa, E., Rozanski, K., Zimnoch, M., Manning, A. C., Leuenberger, M., Uglietti, C., Dolman, A. J., Ciais, P., Heimann, M., and Tans, P. P.: Seven Years of Recent European Net Terrestrial Carbon Dioxide Exchange Constrained by Atmospheric

Observations. *Global Change Biology* 16 (4): 1317–1337. doi:10.1111/j.1365-2486.2009.02078.x, 2010.

Peylin P., P. Rayner, P. Bousquet, C. Carouge, F. Hourdin, P. Heinrich, P. Ciais, and AEROCARB contributors, Daily CO<sub>2</sub> flux over Europe from continuous atmospheric measurements: 1, inverse methodology, *Atmos. Chem. and Phys.*, 5, 3173-3186, ISI:000233610300001, 2005.

Rayner, P. J., Law, R. M., Allison, C. E., Francey, R. J., Trudinger, C. M., and Pickett-Heaps, C.: Interannual variability of the global carbon cycle (1992–2005) inferred by inversion of atmospheric CO<sub>2</sub> and d<sup>13</sup>CO<sub>2</sub> measurements, *Global Biogeochem. Cycles*, 22, GB3008, doi:10.1029/2007GB003068, 2008.

Rödenbeck, C., Estimating CO<sub>2</sub> sources and sinks from atmospheric mixing ratio measurements using a global inversion of atmospheric transport, Technical Report 6, Max Planck Institute for Biogeochemistry, Jena, [http://www.bgc-jena.mpg.de/uploads/Publications/TechnicalReports/tech\\_report6.pdf](http://www.bgc-jena.mpg.de/uploads/Publications/TechnicalReports/tech_report6.pdf), 2005.

Sitch, S., Huntingford, C., Gedney, N., Levy, P. E., Lomas, M., Piao, S., Betts, R., Ciais, P., Cox, P., Friedlingstein, P., Jones, C. D., Prentice, I. C., and Woodward, F. I.: Evaluation of the terrestrial carbon cycle, future plant geography, and climate-carbon cycle feedbacks using 5 Dynamic Global Vegetation Models (DGVMs). *Global Change Biology*, 14 1-25, doi:10.1111/j.1365-2486.2008.01626.x, 2008.

Takahashi, T., Sutherland, S. C., Sweeney, C., Poisson, A., Metzl, N., Tillbrook, B., Bates, N., Wanninkhof, R., Feely, R. A., Sabine, C., Olafsson, J., and Nojiri, Y.: Global sea-air CO<sub>2</sub> flux based on climatological surface ocean pCO<sub>2</sub>, and seasonal biological and temperature effects, *Deep-Sea Res. II*, 49, 1601-1622, 2002.

Takahashi, T., Sutherland, S. C., Wanninkhof, R., Sweeney, C., Feely, R. A., Chipman, D. W., Hales, B., Friederich, G., Chavez, F., Sabine, C., Watson, A., Bakker, D. C. E., Schuster, U., Metzl, N., Yoshikawa-Inoue, H., Ishii, M., Midorikawa, T., Nojiri, Y., Kortzinger, A., Steinhoff, T., Hoppema, M., Olafsson, J., Arnarson, T. S., Tillbrook, B., Johannessen, T., Olsen, A., Bellerby, R., Wong, C. S., Delille, B., Bates, N. R., and de Baar, H. J. W.: Climatological mean and decadal change in surface ocean pCO<sub>2</sub> and net sea-air CO<sub>2</sub> flux over the global oceans. *Deep-Sea Res. II*, 56, 554-577, doi:10.1016/j.dsr2.2008.12.009, 2009.